Leakage Inductances Influences of Integrated-Transformer in Input-Series Flyback Converter

Shengze Liu , Wentao Huang , Tao Meng * , Honggi Ben , Chunyan Li

Posted Date: 3 December 2025

doi: 10.20944/preprints202512.0366.v1

Keywords: flyback integrated-transformer; input-series; leakage inductances; windings layout

 doi:10.20944/preprints202512.0366.v1

Article

Leakage Inductances Influences of Integrated-Transformer in Input-Series Flyback Converter

Shengze Liu [1], Wentao Huang [1], Tao Meng [1,*], Hongqi Ben [2] and Chunyan Li [1]

[1] School of Mechanical and Electrical Engineering, Heilongjiang University, Harbin 150080, China

[2] School of Electrical Engineering and Automation, Harbin Institute of Technology, Harbin 150001, China

* Correspondence: mengtao@hlju.edu.cn

Abstract

In this paper, the leakage inductances influences of integrated-transformer are investigated for an input-series flyback converter, in which each input-series circuit is based on the single-switch flyback topology. First, configuration of this converter is introduced, and a novel multiple inductors coupling model is proposed for its flyback integrated-transformer. Second, operational process of this converter is analyzed considering the leakage inductances between primary and secondary windings of its integrated-transformer. Third, influences of these leakage inductances are analyzed, on this basis, the essential design considerations of flyback integrated-transformer are summarized. Finally, an experimental prototype of this input-series converter is built, based on which, the analysis is verified by the experimental comparisons among three flyback integrated-transformers with various windings layouts.

Keywords: flyback integrated-transformer; input-series; leakage inductances; windings layout

1. Introduction

With the continuous development of power electronics technique, more and more converters with medium or high input voltages (≥1000V) are needed in various industry applications, especially in the renewable energy and transportation applications [1–3]. In these converters, the high voltage issue of each component is the most urgent problem to be solved. The input-series structure is an valid scheme to solve the high voltage problem in the converters with medium or high input voltages, and voltage stress of each component in these converters can be reduced substantially as long as the input voltage sharing of each input-series circuit is achieved [4,5].

Generally, there are two basic input-series structures, one is the output-parallel strategy, as shown in Figure 1a, and the other one is the output-series strategy, as shown in Figure 1b. In addition to the input voltage sharing, the output voltage and current sharing should also be ensured in these two kinds input-series converters respectively [5–7]. In the past years, many voltage or current sharing strategies have been implemented, and a good voltage or current sharing effect can be achieved for each converter [7–12]. These two basic input-series structures can be applied in various power applications, provided the suitable circuit topology is adopted in each input-series circuit. However, their output connections will become more complex when the multiple-output is required, so these two basic input-series structures are not suitable to be applied in the multiple-output applications.

Aiming at the multiple-output applications, the output-independent strategy is applied in the input-series converters, as shown in Figure 1c. The input voltage sharing effect of these converters will be serious when the energies transferring through various output circuits are unbalanced, so the output-independent strategy can only be adopted in the applications when the energies transferring through different output circuits are balanced [13–16].

In addition to the output-parallel, output-series and output-independent strategies, the transformer-integration strategy can also be applied in the input-series converters, as shown in Figure

 doi:10.20944/preprints202512.0366.v1

1d, where all input-series circuits enjoy a common integrated-transformer, so the output circuits can be made in secondary sides of this integrated-transformer conveniently [17–22]. In these input-series transformer-integration (ISTI) converters, the natural input voltage sharing can be achieved, provided all input-series circuits are operating synchronously. The transformer-integration strategy can also be applied in various power applications, as long as the suitable circuit topology is adopted in each input-series circuit. Compared to the output-parallel or output-series strategy, the transformer-integration strategy is much more suitable to be applied when the multiple output circuits are required, which is a conventional requirement in the low power applications.

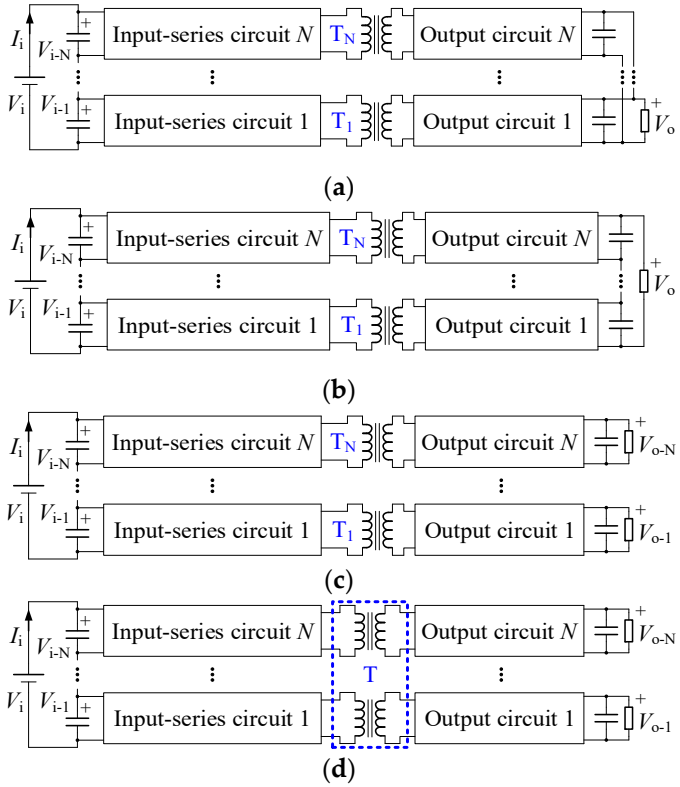

Figure 1. Input-series structures. (a) Output-parallel strategy. (b) Output-series strategy. (c) Output-independent strategy. (d) Transformer-integration strategy.

Recently, the ISTI flyback converters have been investigated systematically in the multiple-output low power applications [18,20]. The investigations show that: input voltage sharing of the ISTI flyback converters can be achieved through the coupling relationships of primary windings in the integrated-transformer, and the input voltage sharing effect cannot be affected by the components in secondary sides of the integrated-transformer. In these ISTI flyback converters, there are multiple primary and secondary windings in each integrated-transformer, influences of the coupling relationships between arbitrary two windings should be clarified, based on which, layouts of these windings can be determined in the design process. Presently, influences of the coupling relationships among primary windings have been clarified, as well as the coupling relationships among secondary windings. However, influences of the coupling relationships between primary and secondary windings have not been clarified.

In each flyback integrated-transformer, there are multiple primary and secondary windings, so numerous leakage inductances are needed to represent the coupling between each primary winding and each secondary winding, which cannot be realized in the existing model of the flyback integrated-transformer. Therefore, a novel multiple inductors coupling model is proposed for this flyback integrated-transformer in this paper, through which the coupling relationships between primary and secondary windings are analyzed, and essential design considerations of the flyback integrated-transformer are summarized.

 doi:10.20944/preprints202512.0366.v1

The remainder of this paper is organized as follows. In section 2, the ISTI flyback converter and multiple inductors coupling model of its integrated-transformer are introduced. In section 3, operational process of this converter is analyzed, where the leakage inductances between primary and secondary windings are considered. In section 4, the leakage inductances influences are analyzed, based on which, essential design considerations of the flyback integrated-transformer are summarized. In section 5, the analysis is verified by the experimental comparisons among three flyback integrated-transformers with various windings layouts. In section 6, the conclusion is given.

2. ISTI Flyback Converter and Its Integrated-Transformer

2.1. Configuration of the ISTI Flyback Converter

Figure 2 shows configuration of the ISTI flyback converter, where each input-series circuit is based on the single-switch flyback topology, V_i and I_i are the input voltage and input current, $V_{i\text{-}1}$, …, $V_{i\text{-}N}$ are input voltages of the N (N≥2) input-series circuits, $V_{o\text{-}1}$, …, $V_{o\text{-}n}$ and $I_{o\text{-}1}$, …, $I_{o\text{-}n}$ are output voltages and output current of the n (n≥1) output-independent circuits.

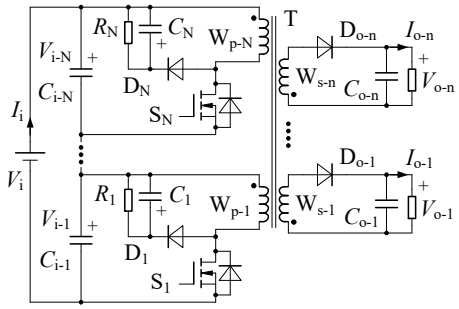

Figure 2. Configuration of the ISTI flyback converter.

In the input-series circuits, there are the identical components and parameters, including the input filter capacitors ($C_{i\text{-}1}$=…=$C_{i\text{-}N}$), the switches (S_1, …, S_N), the turns number ($N_{p\text{-}1}$=…=$N_{p\text{-}N}$) and the self-inductances ($L_{p\text{-}1}$=…=$L_{p\text{-}N}$) of primary windings ($W_{p\text{-}1}$, …, $W_{p\text{-}N}$) in the integrated-transformer (T), and the absorbing circuits (R_1=…=R_N, C_1=…=C_N and D_1, …, D_N).

In the output-independent circuits, the turns number ($N_{s\text{-}1}$, …, $N_{s\text{-}n}$) of secondary windings ($W_{s\text{-}1}$, …, $W_{s\text{-}n}$) in T, as well as the output rectifier diodes ($D_{o\text{-}1}$, …, $D_{o\text{-}n}$) and output filter capacitors ($C_{o\text{-}1}$, …, $C_{o\text{-}n}$) are designed according to the special output requirements.

2.2. Multiple Inductors Coupling Model of Flyback Integrated-Transformer

In [18,20], the input voltage sharing effects of various flyback ISTI converters are investigated. These investigations can be concluded as follows.

(1) The N primary windings of T are considered as a coupled-inductor, by which input voltage sharing of the N input-series circuits is ensured naturally, provided all switches are turning synchronously. The input voltage sharing will be achieved more efficiently as the coupling coefficients of this coupled-inductor increase.

(2) Due to the inevitable parameters errors, the absolute synchronous turning of S_1, …, S_N cannot be realized, so the input voltage differences occur among various input-series circuits, which will increase as the parameters errors increase. The input voltage differences can be reduced through special design of the key parameters, especially the input filter capacitances ($C_{i\text{-}1}$, …, $C_{i\text{-}N}$).

(3) Input voltage sharing effects of the N input-series circuits cannot be affected by the components in secondary sides of T. Influences of the coupling relationships among secondary windings of T are similar to those in the other traditional flyback converters with multiple output circuits, which are not the specific problems in each ISTI flyback converter.

 doi:10.20944/preprints202512.0366.v1

From the above conclusions, it can be obtained that: the flyback integrated-transformer is a main device, so its design and manufacturing are very important.

In the integrated-transformer, there are N primary windings and n secondary windings, so influences of the coupling relationships among these windings should be clarified, on this basis, layouts of these windings can be determined in the design process. In the previous investigations, influences of the coupling relationships among primary windings have been clarified, as well as the coupling relationships among secondary windings. However, influences of the coupling relationships between primary and secondary windings have not been clarified.

Generally, the coupling between arbitrary two windings should be represented by at least one leakage inductance, so $N \times n$ leakage inductances are needed to represent the coupling between N primary windings and n secondary windings, which cannot be realized in the existing model of the flyback integrated-transformer.

To overcome the shortcomings of the existing model, a novel multiple inductors coupling model is proposed for this flyback integrated-transformer, as shown in Figure 3, through which influences of the coupling relationships between primary and secondary windings are expected to be clarified. This novel model is introduced as follows.

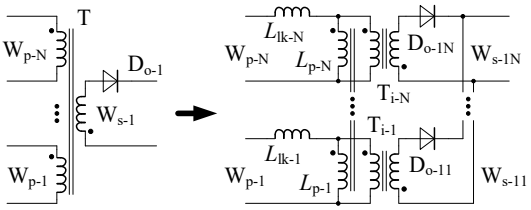

Figure 3. Multiple inductor coupling model of the flyback integrated-transformer.

(1) Influences of the coupling relationships among secondary windings are not considered. To simplify the analysis, the equivalent single secondary winding ($W_{s\text{-}1}$) is adopted to represent the n secondary windings.

(2) The single secondary winding ($W_{s\text{-}1}$) is divided into N identical parts ($W_{s\text{-}11}$, …, $W_{s\text{-}1N}$), and they are made as the secondary windings of the ideal transformers ($T_{i\text{-}1}$, …, $T_{i\text{-}N}$). $T_{i\text{-}1}$, …, $T_{i\text{-}N}$ are connected in parallel in the secondary sides, where their turns ratio are identical ($N_{p\text{-}1}/N_{s\text{-}1}$), and $D_{o\text{-}11}$, …, $D_{o\text{-}1N}$ stand for the output rectifier diodes.

(3) A coupled-inductor ($L_{p\text{-}1}$=…=$L_{p\text{-}N}$) is adopted to represent the coupling relationships among the N primary windings.

(4) The leakage inductances ($L_{lk\text{-}1}$, …, $L_{lk\text{-}N}$) are adopted to represent the coupling relationships between the N primary windings ($W_{p\text{-}1}$, …, $W_{p\text{-}N}$) and the equivalent single secondary winding ($W_{s\text{-}1}$) respectively.

3. Operational Process of ISTI Flyback Converter Considering the Leakage Inductances

Based on the model in Figure 3, operational process of the ISTI flyback converter is analyzed as follows. To simplify the analysis, the following conditions are assumed: 1) this converter operates in discontinuous current mode (DCM); 2) this converter is composed of two input-series circuits (N=2) and single output circuit (n=1); 3) in addition to the integrated-transformer, all devices in this converter are ideal; 4) the asynchronous turning of S_1 and S_2 is not considered; 5) the input voltage differences between two input-series circuits are not considered ($V_{i\text{-}1}$=$V_{i\text{-}2}$=V_i/2); and 6) C_1, C_2 and $C_{o\text{-}1}$ are large enough, so the fluctuations of their voltages (V_{C1}, V_{C2} and $V_{o\text{-}1}$) are ignored. During each switching period, there are the following four stages, where the main waveforms in each period are shown in Figure 4, and the equivalent circuit in each stage is shorn in Figure 5.

Stage 1 (t_0~t_1): At t_0, S_1 and S_2 are turned on. After t_0, the coupled-inductor ($L_{p\text{-}1}$, $L_{p\text{-}2}$) is charged by the input voltages, so its current increases. In the absorbing circuits, D_1 and D_2 are turning off, C_1

 doi:10.20944/preprints202512.0366.v1

and C_2 are discharged through R_1 and R_2 respectively. In the output circuits, $D_{o\text{-}11}$ and $D_{o\text{-}12}$ are turning off, and $I_{o\text{-}1}$ is only provided by $C_{o\text{-}1}$. In this stage, the voltages in primary or secondary side of $T_{i\text{-}1}$ and $T_{i\text{-}2}$ are: $V_{p\text{-}1}=V_{i\text{-}1}=V_i/2$, $V_{p\text{-}2}=V_{i\text{-}2}=V_i/2$ and $V_{s\text{-}11}=V_{s\text{-}12}=N_{s\text{-}1}V_i/2N_{p\text{-}1}$. At t_1, the current of these inductors increases to the peak value during the whole period, as shown in Equation (1).

$$i_{p\text{-}1}(t_1)=i_{p\text{-}2}(t_1)=i_{lk\text{-}1}(t_1)=i_{lk\text{-}2}(t_1)=\int_{t_0}^{t_1}\frac{V_i}{L_{p\text{-}es}}dt \tag{1}$$

where $i_{p\text{-}1}$ (or $i_{p\text{-}2}$) and $i_{lk\text{-}1}$ (or $i_{lk\text{-}2}$) are the current of $L_{p\text{-}1}$ (or $L_{p\text{-}2}$) and $L_{lk\text{-}1}$ (or $L_{lk\text{-}2}$) respectively; $L_{p\text{-}es}=2(1+k_{12})L_{p\text{-}1}$ is the equivalent series inductance of $L_{p\text{-}1}$ and $L_{p\text{-}2}$; k_{12} is the coupling coefficient between $L_{p\text{-}1}$ and $L_{p\text{-}2}$; and $L_{lk\text{-}1}$ (or $L_{lk\text{-}2}$) is much smaller than $L_{p\text{-}es}$, which are not considered here.

Stage 2 (t_1~t_2): At t_1, S_1 and S_2 are turned off, and their voltages (V_{S1} and V_{S2}) increase immediately to $V_{i\text{-}1}+V_{C1}$ and $V_{i\text{-}2}+V_{C2}$ respectively. Duration of these processes are very small, which are not considered here.

After t_1, $D_{o\text{-}11}$ and $D_{o\text{-}12}$ are turning on, and the energies stored in $L_{p\text{-}1}$ and $L_{p\text{-}2}$ are transferred to the loads through $T_{i\text{-}1}$ and $T_{i\text{-}2}$ respectively. In the absorbing circuits, D_1 and D_2 are turning on, and the energies stored in $L_{lk\text{-}1}$ and $L_{lk\text{-}2}$ are transferred into C_1 and C_2 respectively. In this stage, $V_{s\text{-}11}=V_{s\text{-}12}=-V_{o\text{-}1}$ and $V_{p\text{-}1}=V_{p\text{-}2}=-N_{p\text{-}1}V_{o\text{-}1}/N_{s\text{-}1}$, moreover, the expressions of $i_{p\text{-}1}$ (or $i_{p\text{-}2}$) and $i_{lk\text{-}1}$, $i_{lk\text{-}2}$ can be obtained in Equations (2) and (3) respectively.

$$i_{p\text{-}1}(t-t_1)=i_{p\text{-}2}(t-t_1)=i_{p\text{-}1}(t_1)-\int_{t_1}^{t}\frac{N_{p\text{-}1}V_{o\text{-}1}}{2N_{s\text{-}1}L_{p\text{-}ep}}dt \tag{2}$$

$$\begin{cases} i_{lk\text{-}1}(t-t_1)=i_{lk\text{-}1}(t_1)-\int_{t_1}^{t}\dfrac{N_{s\text{-}1}V_{C1}-N_{p\text{-}1}V_{o\text{-}1}}{N_{s\text{-}1}L_{lk\text{-}1}}dt \\ i_{lk\text{-}2}(t-t_1)=i_{lk\text{-}2}(t_1)-\int_{t_1}^{t}\dfrac{N_{s\text{-}1}V_{C2}-N_{p\text{-}1}V_{o\text{-}1}}{N_{s\text{-}1}L_{lk\text{-}2}}dt \end{cases} \tag{3}$$

where $L_{p\text{-}ep}=(1+k_{12})L_{p\text{-}1}/2$ is the equivalent parallel inductance of $L_{p\text{-}1}$ and $L_{p\text{-}2}$.

At the end of this stage, $i_{lk\text{-}1}$ and $i_{lk\text{-}2}$ decrease to zero, and then, D_1 and D_2 are turned off accordingly.

Stage 3 (t_2~t_3): At t_2, $i_{lk\text{-}1}=i_{lk\text{-}2}=0$. After t_2, C_1 (or C_2) is still discharged through R_1 (or R_2), and the decreasing of $i_{p\text{-}1}$ (or $i_{p\text{-}2}$) is continuous. In this stage, $V_{p\text{-}1}$, $V_{p\text{-}2}$ and $V_{s\text{-}11}$, $V_{s\text{-}12}$ are fixed, however, V_{S1} and V_{S2} are changed into $V_{i\text{-}1}+V_{p\text{-}1}$ and $V_{i\text{-}2}+V_{p\text{-}2}$ respectively.

Stage 4 (t_3~t_4): At t_3, $i_{p\text{-}1}=i_{p\text{-}2}=0$. After t_3, $D_{o\text{-}11}$ and $D_{o\text{-}12}$ are turning off, $V_{p\text{-}1}=V_{p\text{-}2}=0$, $V_{s\text{-}11}=V_{s\text{-}12}=0$, $V_{S1}=V_{i\text{-}1}=V_i/2$, $V_{S2}=V_{i\text{-}2}=V_i/2$, and $I_{o\text{-}1}$ is only provided by $C_{o\text{-}1}$.

At t_4, S_1 and S_2 are turned on again. After t_4, this converter will operate in the next period.

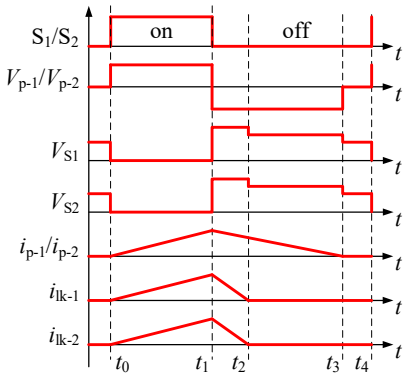

Figure 4. Main voltage and current waveforms in each period.

 doi:10.20944/preprints202512.0366.v1

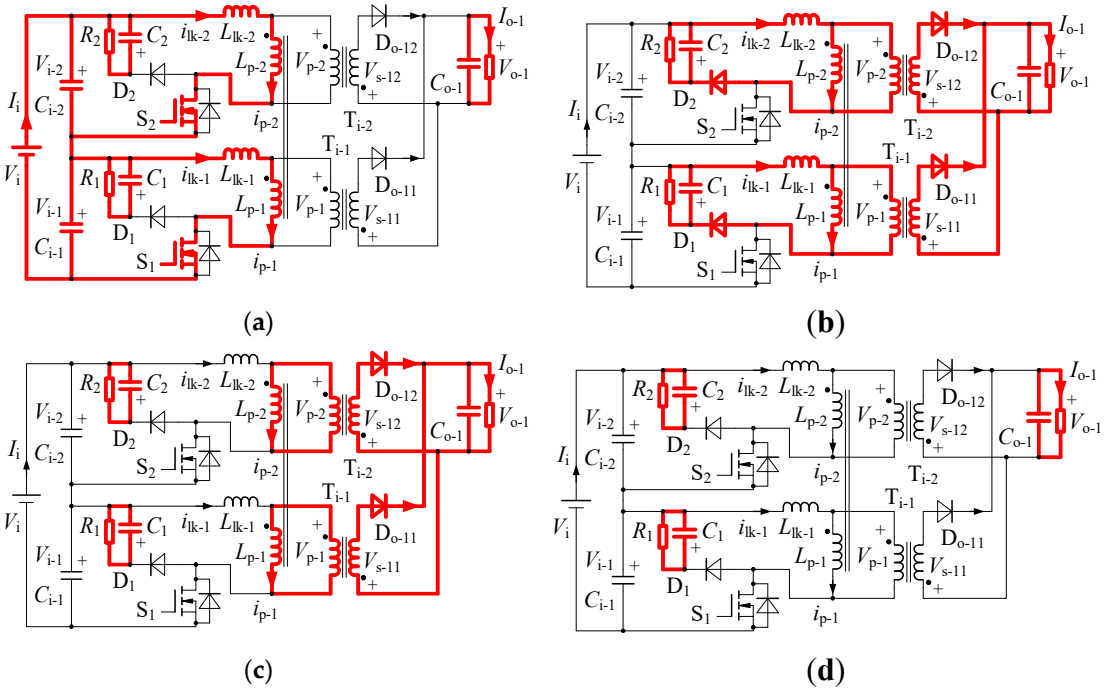

Figure 5. Equivalent circuit in each stage. (a) Stage 1. (b) Stage 2. (c) Stage 3. (d) Stage 4.

4. Design Considerations of Integrated-Transformer Based on the Leakage Inductances

According to the operational process, the influences of leakage inductances ($L_{lk\text{-}1}$, $L_{lk\text{-}2}$) between the primary windings ($W_{p\text{-}1}$, $W_{p\text{-}2}$) and the equivalent single secondary winding ($W_{s\text{-}1}$) are analyzed in this section, based on which, the essential design considerations of this flyback integrated-transformer are summarized.

4.1. Analysis of the Leakage Inductances Influences

For the ISTI flyback converter, the input voltage sharing of each input-series circuit is achieved by the coupling of primary windings in the integrated-transformer, and this input voltage sharing process occurs when all switches are turning on. During the whole switching period, the maximum voltages of S_1 and S_2 are equal to $V_{i\text{-}1}+V_{C1}$ and $V_{i\text{-}2}+V_{C2}$ respectively. Therefore, the voltage sharing effect of S_1 and S_2 cannot be ensured even if a good input voltage sharing effect has been achieved ($V_{i\text{-}1}=V_{i\text{-}2}=V_i/2$).

In stage 1, S_1 and S_2 are turning on, and the coupling relationships of two primary windings ($W_{p\text{-}1}$, $W_{p\text{-}2}$) are represented by the coupled-inductor ($L_{p\text{-}1}$, $L_{p\text{-}2}$). The leakage inductance $L_{lk\text{-}1}$ (or $L_{lk\text{-}2}$) is much smaller than the equivalent series inductance ($L_{p\text{-}es}$) of this coupled-inductor, so the input voltage sharing process in this stage have almost no relationship with $L_{lk\text{-}1}$ (or $L_{lk\text{-}2}$). In stage 3 and stage 4, the current of $L_{lk\text{-}1}$ (or $L_{lk\text{-}2}$) is zero, so there is almost no influence caused by $L_{lk\text{-}1}$ (or $L_{lk\text{-}2}$) in these stages.

Therefore, the analysis of leakage inductances ($L_{lk\text{-}1}$, $L_{lk\text{-}2}$) influences is implemented in stage 2 as follows, where the simplified equivalent circuit of the ISTI flyback converter in stage 2 is shown in Figure 6.

 doi:10.20944/preprints202512.0366.v1

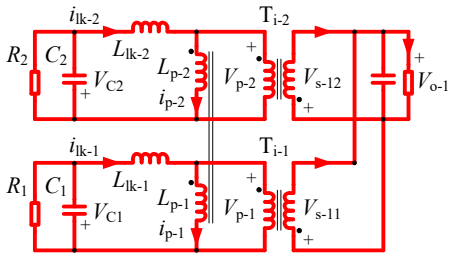

Figure 6. Simplified equivalent circuit of the ISTI flyback converter in stage 2 (V_{s-11}=V_{s-12}= -V_{o-1} and V_{p-1}=V_{p-2}= -$N_{p-1}V_{o-1}/N_{s-1}$).

From operational process of the ISTI flyback converter, it can be obtained that: during the whole switching period, C_1 and C_2 are discharged through R_1 and R_2 respectively. Accordingly, the energies decreasing of C_1 and C_2 during each switching period can be estimated in Equation (4).

$$\begin{cases} E_{C1-} = \dfrac{V_{C1}^2 T}{R_1} \\ E_{C2-} = \dfrac{V_{C2}^2 T}{R_2} \end{cases} \tag{4}$$

where T is the switching period.

It can be obtained from Equation (4) that: when the parameters (R_1=R_2 and C_1=C_2) are fixed, the power losses caused by the absorbing circuit in each input-series circuit is determined by V_{C1} (or V_{C2}), which will increase as V_{C1} (or V_{C2}) increases.

In stage 2, the current of L_{lk-1} and L_{lk-2} will decrease to zero, and their current decreasing durations can be obtained from Equation (3), as shown in Equation (5).

$$\begin{cases} T_{lk-1} = \dfrac{N_{s-1}L_{lk-1}i_{lk-1}(t_1)}{N_{s-1}V_{C1} - N_{p-1}V_{o-1}} \\ T_{lk-2} = \dfrac{N_{s-1}L_{lk-2}i_{lk-2}(t_1)}{N_{s-1}V_{C2} - N_{p-1}V_{o-1}} \end{cases} \tag{5}$$

From Equations (3) and (5), the energies increasing of C_1 and C_2 in stage 2 can be estimated in Equation (6), where T_{lk-1} (or T_{lk-2}) is much smaller than T, so the energies releasing of R_1 and R_2 are not considered in the estimations.

$$\begin{cases} E_{C1+} = \int_{t_1}^{t_1+T_{lk-1}} V_{C1}i_{lk-1}(t-t_1)\mathrm{d}t = \dfrac{N_{s-1}L_{lk-1}V_{C1}\left[i_{lk-1}(t_1)\right]^2}{2\left(N_{s-1}V_{C1} - N_{p-1}V_{o-1}\right)} \\ E_{C2+} = \int_{t_1}^{t_1+T_{lk-2}} V_{C2}i_{lk-2}(t-t_1)\mathrm{d}t = \dfrac{N_{s-1}L_{lk-1}V_{C1}\left[i_{lk-1}(t_1)\right]^2}{2\left(N_{s-1}V_{C1} - N_{p-1}V_{o-1}\right)} \end{cases} \tag{6}$$

During the whole switching period, it is required that: E_{C1+}=E_{C1-} and E_{C2+}=E_{C2-} Therefore, the relationships in Equation (7) can be obtained from Equations (4) and (6).

$$\begin{cases} V_{C1}\left(V_{C1} - \dfrac{N_{p-1}}{N_{s-1}}V_{o-1}\right) = \dfrac{R_1L_{lk-1}\left[i_{lk-1}(t_1)\right]^2}{2T} \\ V_{C2}\left(V_{C2} - \dfrac{N_{p-1}}{N_{s-1}}V_{o-1}\right) = \dfrac{R_2L_{lk-2}\left[i_{lk-2}(t_1)\right]^2}{2T} \end{cases} \tag{7}$$

In stage 2, the energies stored in L_{lk-1} and L_{lk-2} are absorbed by C_1 and C_2, so it should be achieved that: V_{C1}>$N_{p-1}V_{o-1}/N_{s-1}$ and V_{C2}>$N_{p-1}V_{o-1}/N_{s-1}$. Moreover, it is considered that: $i_{lk-1}(t_1)$=$i_{lk-2}(t_1)$, as shown in

 doi:10.20944/preprints202512.0366.v1

Equation (1). Therefore, it can be obtained from Equation (7) that: when the parameters (R_1=R_2 and C_1=C_2) are fixed, V_{C1} and V_{C2} are determined by $L_{lk\text{-}1}$ and $L_{lk\text{-}2}$, which will increase as $L_{lk\text{-}1}$ and $L_{lk\text{-}2}$ increase respectively.

4.2. Essential Design Considerations of Flyback Integrated-Transformer

From the leakage inductances influences, essential design considerations of the flyback integrated-transformer can be summarized from two aspects: 1) voltage sharing effects of the switches (S_1, S_2); and 2) power losses caused by the absorbing circuit in each input-series circuit. They are summarized as follows.

(1) The maximum voltages of S_1 and S_2 are equal to $V_{i\text{-}1}$+V_{C1} and $V_{i\text{-}2}$+V_{C2} respectively. When a good input voltage sharing effect is achieved ($V_{i\text{-}1}$=$V_{i\text{-}2}$=V_i/2) after optimal design of the coupling between primary windings, the voltage sharing effect of C_1 and C_2 should be considered specially. As shown in Equation (7), V_{C1} and V_{C2} are determined by the leakage inductances ($L_{lk\text{-}1}$ and $L_{lk\text{-}2}$), and V_{C1}=V_{C2} can be achieved when $L_{lk\text{-}1}$=$L_{lk\text{-}2}$. Therefore, to achieve a good voltage sharing effect of S_1 and S_2, the difference between $L_{lk\text{-}1}$ and $L_{lk\text{-}2}$ should be suppressed, and $L_{lk\text{-}1}$=$L_{lk\text{-}2}$ is expected to be achieved especially.

(2) The energies stored in $L_{lk\text{-}1}$ and $L_{lk\text{-}2}$ are transferred into C_1 and C_2 in stage 2, and these energies are released through R_1 and R_2 respectively, so these energies should be reduced, which is similar to the other flyback converter. As shown in Equations (4) and (7), the power losses caused by the absorbing circuits will increase as V_{C1} (or V_{C2}) increases, and V_{C1} (or V_{C2}) will increase as $L_{lk\text{-}1}$ (or $L_{lk\text{-}2}$) increases. Therefore, the leakage inductances ($L_{lk\text{-}1}$ and $L_{lk\text{-}2}$) should be reduced to decrease the power losses caused by the absorbing circuits.

5. Experimental Verifications

5.1. Experimental Prototype

To verify the aforementioned analysis, a 1000 V experimental prototype of the ISTI flyback converter is built, as shown in Figure 7. This experimental prototype is composed of two input-series circuits (N=2) and two output-independent circuit (n=2), and each input-series circuit is based on the single-switch flyback topology. The main components and parameters of this experimental prototype are shown in Table 1.

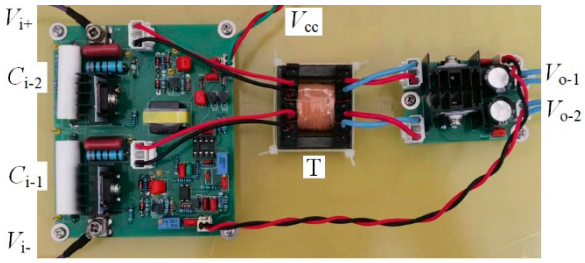

Figure 7. Experimental prototype of the ISTI flyback converter.

Table 1. Components and parameters of the prototype.

Components or parameters	Features or values
V_i	1000 V (N=2)
$V_{o\text{-}1}$, $V_{o\text{-}2}$	24V ($V_{o\text{-}1}$=$V_{o\text{-}2}$, n=2)
$I_{o\text{-}1}$, $I_{o\text{-}2}$	1.5 A, 1 A
$C_{i\text{-}1}$, $C_{i\text{-}2}$	1200 V/0.1 μF ($C_{i\text{-}1}$=$C_{i\text{-}2}$)
S_1, S_2	2SK1271 (T=20 μs)
$D_{o\text{-}1}$, $D_{o\text{-}2}$	MUR1560
$C_{o\text{-}1}$, $C_{o\text{-}2}$	50 V/1000 μF ($C_{o\text{-}1}$=$C_{o\text{-}2}$)

 doi:10.20944/preprints202512.0366.v1

R_1, R_2	15 kΩ (R_1=R_2)
C_1, C_2	630 V/0.1 μF (C_1=C_2)
D_1, D_2	BYV26G

Based on this prototype, three flyback integrated-transformers (T_1, T_2 and T_3) with various typical layout schemes of the primary windings (W_{p-1}, W_{p-2}) are designed for the experimental comparisons. Windings layouts of T_1, T_2 and T_3 can be obtained from their cross sections, as shown in Figure 8, in which only half of the cross section is given in each illustration, and the number marked on each turn represents its manufacturing sequence.

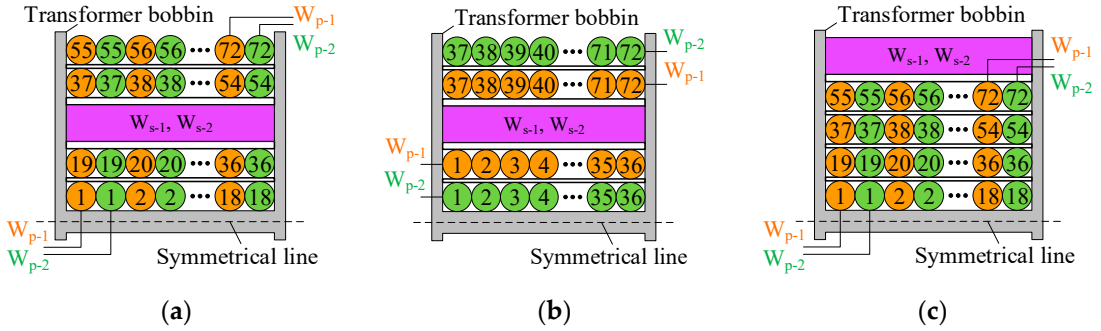

Figure 8. Cross sections of the flyback integrated-transformer. (a) The illustration of T_1. (b) The illustration of T_2. (c) The illustration of T_3.

In each flyback integrated-transformer, the secondary windings (W_{s-1}, W_{s-2}) are connected in parallel, and they are manufactured intensively to improve their coupling relationship. Layouts of W_{s-1} and W_{s-2} are identical in T_1, T_2 and T_3, which are not given specially in Figure 8. Moreover, the other common features of these integrated-transformers are shown in Table 2, and layout schemes of their primary windings (W_{p-1}, W_{p-2}) are explained as follows.

In T_1, W_{p-1} and W_{p-2} are connected in parallel. The four layers of W_{p-1} and W_{p-2} are divided into two parts, where W_{s-1} and W_{s-2} are rounded in the middle of these two parts.

In T_2, the layer-by-layer windings layout is selected for W_{p-1} and W_{p-2}. The two layers of W_{p-1} (or W_{p-2}) are divided into two parts, where W_{s-1} and W_{s-2} are rounded in the middle of these two parts. The two layers of W_{p-1} are rounded near W_{s-1} and W_{s-2}, and the two layers of W_{p-2} are rounded in the innermost and outermost layers respectively.

In T_3, W_{p-1} and W_{p-2} are connected in parallel, and they are made in the inner four layers. W_{s-1} and W_{s-2} are made in the outer layers.

Table 2. Common features of the integrated-transformers.

Types or parameters	Features or values
Magnetic core	EI 40 (Ferroxcube)
N_{p-1}, N_{p-2}	72 (N_{p-1}=N_{p-2})
N_{s-1}, N_{s-2}	14 (N_{s-1}=N_{s-2})
L_{p-1}, L_{p-2}	1.36 mH (L_{p-1}=L_{p-2})
Layer number (W_{p-1}, W_{p-2})	4

The main parameters of these integrated-transformers are measured by the *LCR* meter (Tonghui/TH2826), including the coupling coefficient (k_{12}) and the leakage inductances (L_{lk-1}, L_{lk-2}). The measuring results are shown in Table 3. It can be obtained that: 1) a high coupling coefficient has been achieved in each integrated-transformer; 2) in T_1 (or T_3), there is almost no difference between L_{lk-1} and L_{lk-2}, however, there is an obvious difference between L_{lk-1} and L_{lk-2} in T_2; and 3) in T_3, L_{lk-1} (or L_{lk-2}) is much larger than that in T_1 (or T_2).

 doi:10.20944/preprints202512.0366.v1

Table 3. Measuring results of the integrated-transformer.

T	T_1	T_2	T_3
k_{12}	0.998999	0.997627	0.999130
L_{lk-1}	13 μH	11 μH	36 μH
L_{lk-2}	13 μH	18 μH	35 μH

According to the aforementioned analysis, the experimental results can be expected that: 1) a good input voltage sharing effect will be achieved for this experimental prototype when any one of the integrated-transformers is adopted; 2) when T_1 (or T_3) is adopted, there is almost no voltage difference between C_1 and C_2, so a good voltage sharing effect will be achieved between S_1 and S_2; 3) when T_1 (or T_2) is adopted, the voltages of C_1 and C_2 will be lower than those when T_3 is adopted; and 4) when T_1 (or T_2) is adopted, the power losses caused by the absorbing circuits will be much lower, so the efficiency of the experimental prototype will be higher than that when T_3 is adopted.

5.2. Experimental Results

The three flyback integrated-transformers (T_1, T_2 and T_3) are used in this experimental prototype one by one, and the main experimental results are shown in Figure 9, Figure 10, Figure 11 and Table 4.

Figure 9 shows the main experimental waveforms when T_1 is used, including the driving (v_{gs1}), voltage (v_{ds1}) and current (i_{S1}) of S_1, the driving (v_{gs2}), voltage (v_{ds2}) and current (i_{S2}) of S_2, the input voltages (V_{i-1}, V_{i-2}) of two input-series circuits, and the voltages (V_{C1}, V_{C2}) of two capacitors in the absorbing circuits. Figure 10 and Figure 11 show the main experimental waveforms when T_2 and T_3 are used. It can be seen from these waveforms that: a good input voltage sharing effect has been achieved for this experimental prototype when any one of the integrated-transformers is adopted.

Table 4 shows the main measuring results when T_1, T_2 and T_3 are used one by one, including the voltages (V_{C1}, V_{C2}) of two capacitors in the absorbing circuits, and the efficiency (η) of this experimental prototype.

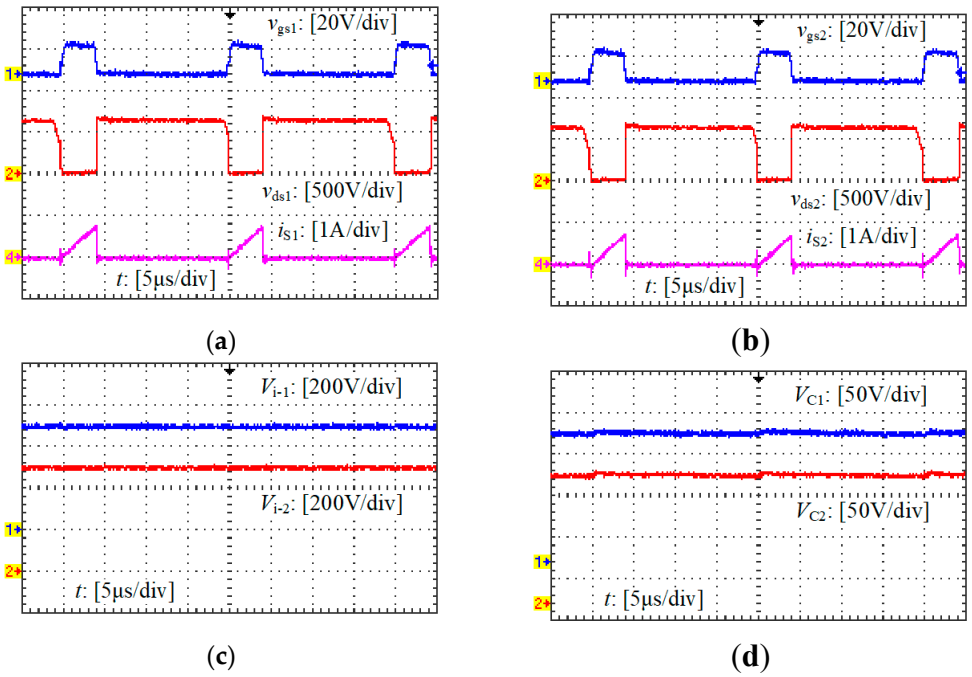

Figure 9. Main waveforms of the prototype when T_1 is used. (a) Voltage and current of S_1. (b) Voltage and current of S_2. (c) Input voltages (V_{i-1}, V_{i-2}). (d) Voltages of C_1 and C_2.

 doi:10.20944/preprints202512.0366.v1

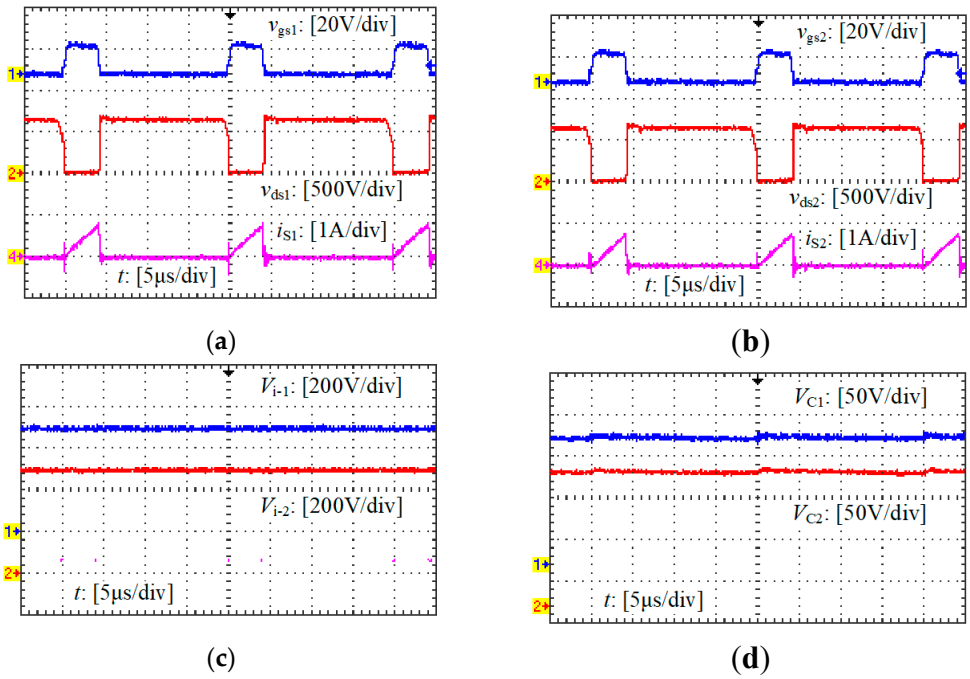

Figure 10. Main waveforms of the prototype when T_2 is used. (a) Voltage and current of S_1. (b) Voltage and current of S_2. (c) Input voltages (V_{i-1}, V_{i-2}). (d) Voltages of C_1 and C_2.

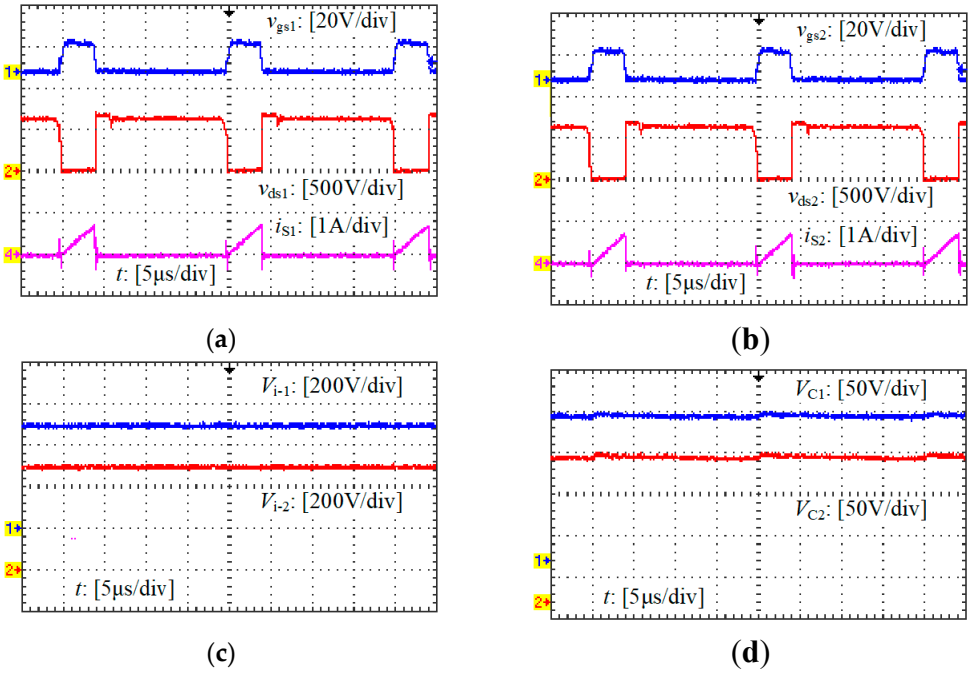

Figure 11. Main waveforms of the prototype when T_3 is used. (a) Voltage and current of S_1. (b) Voltage and current of S_2. (c) Input voltages (V_{i-1}, V_{i-2}). (d) Voltages of C_1 and C_2.

Table 4. Main measuring results.

T	T_1	T_2	T_3
V_{C1}	155 V	152 V	175 V
V_{C2}	155 V	161 V	175 V
η	87.12%	87.01%	83.78%

It can be obtained from Figure 9d, Figure 10d, Figure 11d and Table 4 that: 1) when T_1 is used, there is almost no voltage difference between the two capacitors (C_1 and C_2) in the absorbing circuits;

 doi:10.20944/preprints202512.0366.v1

2) when T_2 is used, an obvious voltage difference (V_{C2}-V_{C1}=9 V) appears between C_1 and C_2; and 3) when T_3 is used, there is almost no voltage difference between C_1 and C_2, however, voltage of C_1 (or C_2) is much higher than that when T_1 (or T_2) is adopted. Moreover, it can also be obtained from Table 4 that: when T_1 (or T_2) is used, the efficiency of this experimental prototype is higher than that when T_3 is adopted.

Therefore, it can be seen that: the analysis of the leakage inductances influences has been verified through the above experimental comparisons.

6. Conclusion

In this paper, influences of the leakage inductances between primary and secondary windings are investigated for the integrated-transformer in an input-series flyback converter, in which each input-series circuit is based on the single-switch flyback topology. To represent the coupling relationship between primary and secondary windings, a novel multiple inductors coupling model is proposed for the flyback integrated-transformer, operational process of this converter and the leakage inductances influences are analyzed based on this model, and the essential design considerations of flyback integrated-transformer are summarized: 1) the difference of various leakage inductances should be suppressed as much as possible to achieve a good voltage sharing effect of the switches in different input-series circuits; and 2) the leakage inductances should be reduced to decrease the power losses of this converter. The investigating results are verified by the experimental comparisons among three flyback integrated-transformers with various windings layouts.

Author Contributions: Conceptualization, S.L. and T.M.; methodology, T.M. and H.B.; software, W.H. and C.L.; validation, S.L. and W.H.; formal analysis, T.M.; investigation, S.L.; resources, T.M.; data curation, S.L. and W.H.; writing—original draft preparation, S.L.; writing—review and editing, S.L. and T.M.; supervision, T.M. and H.B.; project administration, T.M.; funding acquisition, T.M. and C.L. All authors have read and agreed to the published version of the manuscript.

Funding: This research was supported by Heilongjiang Provincial Natural Science Foundation of China (LH2023E107), Program for Young Talents of Basic Research in Universities of Heilongjiang Province (YQJH2024181), and Heilongjiang University Fundamental Research Funds for the Heilongjiang Province Universities (2024-KYYWF-0114).

Data Availability Statement: Data are provided within the manuscript.

Conflicts of Interest: The authors declare no conflicts of interest.

References

1. Yoon, D.; Cho, Y.; Bae, S.; Lee, J. An input-series output-series noninverting buck-boost converter for 1500 V dc bus with wide input and output voltage ranges. *IEEE Trans. Ind. Electron*. 2023, 70, 11231–11241.
2. Ren, X.; Xu, Z.; Zhang, Z.; Li, H.; He, M.; Tang, J.; Chen, Q. A 1-kV input SiC LLC converter with split resonant tanks and matrix transformers. *IEEE Trans. Power Electron*. 2019, 34, 10446–10457.
3. Chen, X.; Chen, W.; Yang, X.; Han, Y.; Hao, X.; Xiao, T. Research on a 4000-V-ultrahigh-input-switched-mode power supply using series-connected MOSFETs. *IEEE Trans. Power Electron*.2018, 33, 5995–6011.
4. Ma, Q.; Huang, Q.; Huang, A. Zero-voltage switching and natural voltage balancing of a 3 kW 1 MHz input-series-output-parallel GaN LLC converter. *IEEE Open J. Power Electron*. 2024, 5, 1119–1128.
5. Ma, D.; Chen, W.; Ruan, X. A review of voltage/current sharing techniques for series-parallel-connected modular power conversion systems. *IEEE Trans. Power Electron*. 2020, 35, 12383–12400.
6. Liu, F.; Zhou, G.; Ruan, X.; Ji, S.; Zhao, Q.; Zhang, X. An input-series-output-parallel converter system exhibiting natural input-voltage sharing and output-current sharing. *IEEE Trans. Ind. Electron*. 2021, 68, 1166–1177.
7. Sha, D.; Guo, Z.; Luo, T.; Liao, X. A general control strategy for input-series-output-series modular dc-dc converters. *IEEE Trans. Power Electron*. 2014, 29, 3766–3775.

 doi:10.20944/preprints202512.0366.v1

8. Qu, L.; Zhang, D.; Zhang, B. Input voltage sharing control scheme for input-series and output-parallel connected dc-dc converters based on peak current control. *IEEE Trans. Ind. Electron*. 2019, 66, 429–439.
9. Wang, L.; Sun, P.; Liang, Y.; Wu, X.; Deng, Q.; Rong, E. Analysis and control design for input-series output-parallel multi-channel inductive power transfer system. *IET Power Electron*. 2024, 17, 2515–2530.
10. Li, S.; Wang, Z.; Yuan, X.; Zhang, Y.; Sun, L.; Wang, K.; Wu, X. A 10 kV/400 V SiC based dc-dc converter with input-series-output-parallel configuration and three-loop control. *IEEE Trans. Ind. Appl*. 2024, 60, 7013–7029.
11. Liu, Y.; Hu, H.; Wang, X.; Gang, Y.; Li, Y. Voltage balance scheme for input-series output-series DAB dc-dc converter with bidirectional power flow. *IEEE Trans. Power Electron*. 2024, 39, 12030–12034.
12. Li, J.; Ma, X.; Xie, Y.; Wang, T.; Shu, Z. Power and voltage balance control strategy of series input parallel output type three-level dual active bridge converter. *Trans. China Elect. Soc*. 2024, 39, 3082–3092.
13. Hu, Q.; Zane, R. LED driver circuit with series-input-connected converter cells operating in continuous conduction mode. *IEEE Trans. Power Electron*. 2010, 25, 574–582.
14. Yang, W.; Zhang, Z.; Yang, S. A new control strategy for input voltage sharing in input series output independent modular dc-dc converters. *J. Power Electron*. 2017, 17, 632–640.
15. Yang, J.; Zhang, Z.; Sun, K.; Yang, W.; Yang, S.; Li, F.; Yao, Y. Series input multiple outputs flyback auxiliary power supply for input series-output parallel/input series-output series system. *IET Power Electron*. 2019, 12, 2285–2294.
16. Liu, Y.; Liu, X.; Gao, F.; Liu, D.; Wheeler, P. Auxiliary power supply for input-series output-parallel medium-voltage solid state transformers. *IEEE Trans. Power Electron*. 2023, 38, 7308–7321.
17. Choi, S.; Lee, J.; Lee, J. High-efficiency portable welding machine based on full-bridge converter with ISOP-connected single transformer and active snubber. *IEEE Trans. Ind. Electron*. 2016, 63, 4868–4877.
18. Meng, T.; Li, C.; Ben, H.; Zhao, J. An input-series flyback auxiliary power supply scheme based on transformer-integration for high-input voltage applications. *IEEE Trans. Power Electron*. 2016, 31, 6383–6393.
19. Meng, T.; Ben, H.; Song, Y.; Li, C. Analysis and design of an input-series two-transistor forward converter for high-input voltage multiple-output applications. *IEEE Trans. Ind. Electron*.2018, 65, 270–279.
20. Meng, T.; Song, Y.; Wang, Z.; Ben, H.; Li, C. Investigation and implementation of an input-series auxiliary power supply scheme for high-input-voltage low-power applications. *IEEE Trans. Power Electron*. 2018, 33, 437–447.
21. Meng, T.; Ben, H.; Song, Y.; Li, C. Analysis and suppression of the circulating current influence in the input-series auxiliary power supply for high-input-voltage applications. *IEEE Trans. Power Electron*. 2019, 34, 6533–6543.
22. Wang, Y.; Kim, S.; Zhang, H.; Chen, Y.; Park, S. Design and analysis of an input-series quasi-resonant flyback high-voltage SMPS based on an integrated transformer. *IET Power Electron*. 2022, 15, 1058–1074.